Electric field effect on the thermal conductivity of wurtzite GaN

Cite as: Appl. Phys. Lett. **118**, 162110 (2021); https://doi.org/10.1063/5.0047372 Submitted: 12 February 2021 • Accepted: 09 April 2021 • Published Online: 22 April 2021

Yujie Quan, 📵 Sheng-Ying Yue and 📵 Bolin Liao







ARTICLES YOU MAY BE INTERESTED IN

Ultrawide bandgap semiconductors

Applied Physics Letters 118, 200401 (2021); https://doi.org/10.1063/5.0055292

Thermal transport properties of GaN with biaxial strain and electron-phonon coupling Journal of Applied Physics 127, 035102 (2020); https://doi.org/10.1063/1.5133105

Phonon properties and thermal conductivity from first principles, lattice dynamics, and the Boltzmann transport equation

Journal of Applied Physics 125, 011101 (2019); https://doi.org/10.1063/1.5064602





Electric field effect on the thermal conductivity of wurtzite GaN

Cite as: Appl. Phys. Lett. 118, 162110 (2021); doi: 10.1063/5.0047372 Submitted: 12 February 2021 · Accepted: 9 April 2021 · Published Online: 22 April 2021







Yujie Quan, Sheng-Ying Yue, 🕞 and Bolin Liao^{a)} 🕞

AFFILIATIONS

Department of Mechanical Engineering, University of California, Santa Barbara, California 93106, USA

a) Author to whom correspondence should be addressed: bliao@ucsb.edu

ABSTRACT

Gallium nitride (GaN), a wide bandgap semiconductor, has been broadly used in power electronic devices due to its high electron mobility and high breakdown voltage. Its relatively high thermal conductivity makes GaN a favorable material for such applications, where heat dissipation is a major concern for device efficiency and long-term stability. However, in GaN-based transistors, where the active region can withstand extremely strong electric fields, the field effect on the thermal transport properties has drawn little attention so far. In this work, we apply first-principles methods to investigate phonon properties of wurtzite GaN in the presence of a near-breakdown electric field applied along different crystallographic directions. We find that the electric field changes thermal conductivity considerably via impacting the bond stiffness, ionicity, anharmonicity, and the crystal symmetry, although it has little effect on phonon dispersions. The presence of an out-ofplane electric field increases (decreases) the thermal conductivity parallel (perpendicular) to the electric field, which is attributed to different changes in the Ga-N bond stiffness and ionicity and the scattering rates of phonons traveling along different directions. When an in-plane electric field is applied, the sizable decrease in thermal conductivities along all directions is attributed to the crystal symmetry breaking that enhances the phonon-phonon scattering. Our study provides insight into the effect of extreme external electric fields on phonon transport properties in wide-gap semiconductors.

Published under license by AIP Publishing. https://doi.org/10.1063/5.0047372

Excellent electronic properties of GaN, such as the wide bandgap and, thus, the high breakdown electric field, as well as the high electron mobility, make it a promising material for high-power and highfrequency applications. 1-3 Due to the extremely high power densities present in GaN-based power electronic devices,4 efficient thermal management is of great importance to maintain the device efficiency and avoid device failure due to large local temperature rises. Extensive experimental and theoretical studies have shown that bulk wurtzite GaN possesses a high thermal conductivity, $^{5-10}$ which is beneficial for heat dissipation in power electronic applications. Recently, new strategies to form high-quality bonds between GaN and high-thermal conductivity substrates with low interfacial thermal resistances have also been developed. However, these thermal transport studies so far have focused on GaN without an external electric field. Given the extreme electric field strength (up to a few MV/cm)^{4,12} present in the active region in GaN-based devices, the impact of the external electric field on the thermal conductivity of GaN is critical to evaluate the thermal performance of operating devices.

The electric field effect on thermal conductivity is not well understood in general. Computationally, recent advances in first-principles methods based on density functional theory (DFT), density functional perturbation theory¹³ (DFPT), and phonon Boltzmann transport equation (BTE) have facilitated the calculation of thermal conductivities of a wide range of crystalline materials under zero electric field. 14,15 However, there have been very few studies on the influence of an external electric field on thermal transport properties. Most of these studies examined two-dimensional (2D) materials in the presence of an out-of-plane electric field. For these studies, slab supercells with a sawtooth potential 16 were used to incorporate finite electric fields. This method is natural for simulating 2D materials but becomes computationally expensive for bulk three-dimensional materials due to the large required supercell size. Qin et al. 17 showed that the thermal conductivity of silicene can be tuned within a wide range, up to two orders of magnitude, with an out-of-plane external electric field that modulates the interactions between atoms. Similar results were also obtained in monolayer borophene by Yang et al. 18 Experimental studies have mostly focused on ferroelectric materials so far. 19,20

The development of the modern theory of polarization, ^{21–23} where an electronic enthalpy functional including an additional polarization term is minimized with respect to polarized Bloch functions,

has provided a practical first-principles method to calculate the response of physical properties to a finite electric field in 3D bulk materials since supercells are not required. In this Letter, we apply this first-principles method to investigate phonon properties of wurtzite GaN in the presence of a near-breakdown electric field applied along different directions. The electric field is applied along both the inplane direction (the a-axis) and the out-of-plane direction (the c-axis), as shown in Fig. 1(a). For both cases, we found considerable changes in the thermal conductivity, up to 24% at 200 K and 13% at 300 K, depending on the directions of the electric field and the thermal conductivity [Figs. 1(c) and 1(d)]. Given the high heat current existing in power electronic devices, this moderate change in thermal conductivity can lead to sizable temperature variation in the device. Through detailed analysis of individual phonon modes, we attributed the change in the thermal conductivity to the combined effect of two major factors: the change in bond ionicity and stiffness and the crystal symmetry breaking due to the applied electric field. The change in bond stiffness and ionicity affects the phonon frequency and group velocity, while the broken crystal symmetry leads to enhanced phonon-phonon scatterings. Our study suggests that the field effect on the thermal conductivity in wide-gap semiconductors needs to be considered in designing thermal management strategies for high-power devices based on these materials.

DFT calculations were performed using the Quantum ESPRESSO (QE) package²⁴ with the scalar-relativistic Optimized Norm-Conserving Vanderbilt (ONCV) pseudopotentials²⁵ within the local density approximation (LDA). The kinetic energy cutoff for wavefunctions is set to 80 Ry. A mesh grid of $10 \times 10 \times 5$ in the first Brillouin zone (BZ) is adopted, and the total electron energy convergence threshold for self-consistency is 1×10^{-10} Ry. The crystal lattice is fully relaxed with a force threshold of 1×10^{-4} eV/Å, with zero-field lattice parameters a = 3.16 Å, c = 5.148 Å and the internal

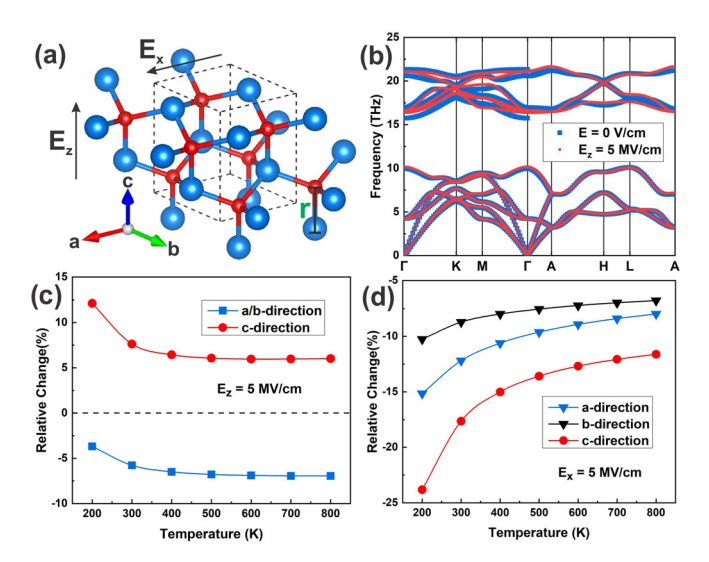


FIG. 1. (a) The crystal structure of wurtzite GaN. The applied electric field directions are labeled. (b) The comparison of phonon dispersions of wurtzite GaN with and without an out-of-plane electric field. (c) and (d): The relative changes in the calculated lattice thermal conductivity along different directions in the presence of (c) out-of-plane and (d) in-plane electric fields.

parameter u = 0.375 (u is the ratio between the Ga–N bond length r along the c-axis and the lattice parameter c), in excellent agreement with experimental values.²⁶ The second- and third-order interatomic force constants (IFCs) were calculated using a finite displacement approach²⁷ with $3 \times 3 \times 2$ supercells with or without the electric field. The phonon dispersions based on the second-order IFCs were calculated using the PHONOPY package,²⁸ and the non-analytical correction term due to the long-range Coulomb interactions was also included. The interactions between atoms were taken into account up to fifth-nearest neighbors in third-order IFC calculations. The phonon-phonon scattering rates and phonon-isotope scattering rates can be computed based on the IFCs, as detailed in previous works.^{5,6} We calculated the lattice thermal conductivity by solving the phonon Boltzmann Transport Equation (BTE) iteratively as implemented in ShengBTE.²⁹ The q-mesh samplings for the BTE calculations were $15 \times 15 \times 15$. The convergence of the lattice thermal conductivity with respect to the q-mesh density and the interaction distance cutoff was confirmed. The finite electric field was applied based on the modern theory of polarization^{21,22} as implemented in QE. Given the 3.4 eV bandgap of the wurtzite GaN, the near-breakdown electric field of 5 MV/cm is applied in the calculation. The crystal structure is fully relaxed with the applied electric field. The change in the lattice parameters a and c with the electric field is described by the inverse piezoelectric coefficients of GaN: $d_{31} = \frac{\partial \ln(a)}{\partial E_z} = -1.37 \times 10^{-4}$ cm/MV and $d_{33} = \frac{\partial \ln(c)}{\partial E_z} = 2.83 \times 10^{-4}$ cm/MV. ¹² Therefore, the change in the lattice parameters is below 0.1% with the applied electric field, which agrees with our calculation. It is noted here that the electric field is also applied during the calculations of second- and third-order IFCs, and therefore, our calculations can capture the full response of phonon properties to the applied electric field, including the effects of both the change in atomic positions and the redistribution of the electronic charge density.²

The comparison of phonon dispersions with and without the applied electric field along the c-axis is shown in Fig. 1(b). A similar plot with the electric field applied along the a-axis is given in Fig. S1 (see the supplementary material). In the presence of the electric field along both the a-axis and the c-axis, the dispersions of low-frequency acoustic phonons are not changed appreciably, while slight changes arise for the high-frequency optical phonons. Our calculated shift of the optical phonon frequencies at the Γ point with an out-of-plane electric field agrees qualitatively with the Raman measurements by Bagnall et al, al where the frequency of A1 (LO) mode increases and that of E2 (high) and E2 (low) modes decreases, validating our calculations incorporating the electric field.

Although the electric field has little effect on the phonon dispersion, it has a much greater impact on the lattice thermal conductivity, as shown in Figs. 1(c) and 1(d). The thermal conductivity of GaN as a function of temperature in zero field is shown in Fig. S2 (see the supplementary material). Both phonon-phonon scattering and phonon-isotope scattering are considered when calculating the thermal conductivity, since it is well known that the phonon-isotope scattering plays a prominent role in GaN.⁵ Our calculated thermal conductivity of isotopically pure GaN is 410 W/mK at 300 K, while the calculated thermal conductivity of GaN with the natural abundance of Ga isotopes is 250 W/mK at 300 K, agreeing well with other first-principles calculations.^{5–7} When the electric field is applied

along the out-of-plane direction, a sizable increase in the thermal conductivity parallel to the electric field is observed, with more than 12% increase at 200 K and 8% at higher temperatures. In contrast, the thermal conductivity perpendicular to the electric field decreases by 7%. On the other hand, when the electric field is applied along the in-plane direction, the in-plane crystal symmetry is broken, which makes the a-axis and the b-axis no longer equivalent. Moreover, the thermal conductivities along all three axes decrease in this case, with the largest reduction reaching 24% at 200 K for the thermal conductivity along the c-axis. The field effect on the thermal conductivity with a lower electric field (1 MV/cm) is provided in Fig. S3 (see the supplementary material).

Since the lattice thermal conductivity can be decomposed into contributions from individual phonon modes,²⁷ we analyze the transport and scattering properties of individual phonon modes to understand the mechanisms underlying the observed field effect. We first examine the case where an out-of-plane electric field is applied. Since the field direction is aligned with the rotational axis (c-axis) of the crystal lattice, the full crystal symmetry of GaN is preserved. The phonon-phonon scattering rates in this case are presented in Fig. 2(a), showing no appreciable difference with or without the applied field. The change in the spectral contribution to the thermal conductivity (Fig. S4) also shows no clear trend for different frequency regimes. To see the change in the scattering rates of phonons traveling along different directions, we plot the change in the phonon scattering rate for groups of phonons mainly contributing to out-of-plane and in-plane thermal transport based on their group velocities, as shown in Fig. 2(b). Although the average total phonon scattering rates appear unchanged, we found that for phonons with a large out-of-plane group velocity, their scattering rates tend to be reduced by the applied electric field, while the phonons with a large in-plane group velocity tend to have an increased scattering rate. This effect would contribute to the observed thermal conductivity change. To quantify the effect, we also calculated the average phonon scattering rates weighted by their cross-plane and inplane group velocities: $\overline{\left(\frac{\Delta \gamma}{\gamma}\right)_{\alpha}} = \frac{\sum_{\text{all modes}} v_{\alpha}^{2} \left(\frac{\Delta \gamma}{\gamma}\right)_{\alpha}}{\sum_{\text{all modes}} v_{\alpha}^{2}}$, where α refers to the

direction and $\frac{\Delta \gamma}{\gamma}$ is the relative change of the scattering rate for a certain

phonon mode. We found $\overline{\left(\frac{\Delta \gamma}{\gamma}\right)_x} = -2\%$ and $\overline{\left(\frac{\Delta \gamma}{\gamma}\right)_z} = 10.8\%$, contributing to the different changes in the lattice thermal conductivity along the two directions.

Then, we focus on the bond length and the bond strength of the Ga-N bonds, as they can influence the harmonic phonon properties, such as the mode-specific heat capacity and the group velocity. The data are summarized in Table I. We notice a slight decrease in the bond length of the out-of-plane Ga-N bond by 0.9% and an increase in the bond length of the in-plane Ga-N bond by 0.3%. The change in the out-of-plane bond length is on the same order as the experimental value. 12 Using second-order polynomial fitting of the total energy as a function of small perturbations (smaller than 0.05 Å) of the bond length, we obtain the stiffness of the in-plane and out-of-plane Ga-N bonds. We find that the stiffness of the outof-plane Ga-N bond is increased by 6.4%, while the stiffness of the in-plane Ga-N bond is decreased by 2.3%. Typically, the increase in the bond stiffness leads to the enhancement of the phonon frequency and the group velocity. Although the change in phonon frequency is not clear in Fig. 1(b), where all phonon modes are displayed, the change is more evident for the phonon modes vibrating along a certain bond direction. The phonon modes vibrating along the out-of-plane direction are selected according to their eigenvectors, and the corresponding phonon frequency and group velocity compared with the zero-field values are shown in Fig. S5 (see the supplementary material). Considering the negligible contribution of high-frequency optical phonons to the thermal conductivity, only phonons with frequencies below 10 THz are shown. It is found that both the out-of-plane group velocities and the frequency of this group of phonons are increased by 2% on average in the presence of the out-of-plane electric field, which are the main contributors to the increased out-of-plane thermal conductivity. In contrast, the frequencies of the phonons with in-plane vibrations are reduced. Although the in-plane group velocities of some of the phonons with in-plane vibrations are slightly increased with the electric field, their frequency lies in the range of 5-7 THz and they are known to be strongly suppressed by phonon-isotope scatterings.

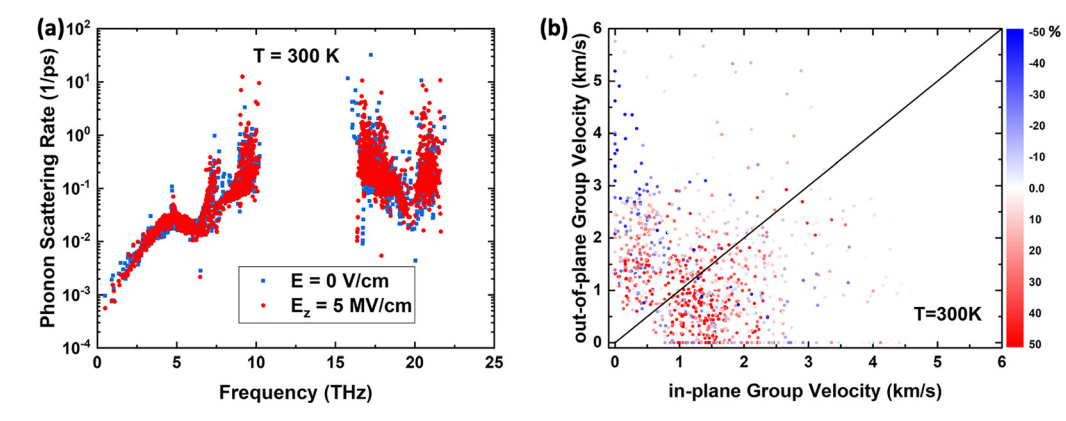


FIG. 2. (a) The phonon–phonon scattering rate at 300 K at zero field (blue spots) and with an out-of-plane 5 MV/cm electric field. (b) Relative change of phonon scattering rates as a function of their in-plane and out-of-plane group velocities. Here, each dot represents a phonon mode, whose coordinates are determined by their cross-plane and in-plane group velocities. The color of the dots represents the relative change in their scattering rates when an out-of-plane electric field is applied. Blue means the decreased scattering rate, while red means an increased scattering rate.

TABLE I. Relative changes of Ga-N bond properties with and without an out-of-plane near-breakdown electric field of 5 MV/cm.

	In-plane Ga–N	In-plane Ga–N	Out-of-plane Ga–N	Out-of-plane Ga–N
	bond length	bond stiffness	bond length	bond stiffness
Relative change	0.3%	-2.3%	-0.9%	6.4%

We also estimated that the change in the phonon heat capacity due to the frequency change is within 0.5%, thus not affecting the thermal conductivity appreciably.

Given that the relative change in the bond stiffness is much greater than that in the bond length, we hypothesize that the change in the bond stiffness in the presence of the electric field is not only a consequence of the change in the bond length but also affected by the redistribution of the charge density, i.e., the ionicity of the Ga–N bonds. The electron localization function (ELF) is often used as a visually informative method to demonstrate the bond ionicity, whose value is normalized between 0 and 1. A higher ELF value at a spatial location indicates a stronger Pauli exclusion to a test electron placed in the proximity, signaling a higher local charge density and bond saturation. Therefore, higher ELF values concentrated in between two ions indicate strong covalent bonding, while low ELF values between the two ions are a signature of highly ionic bonds. The ELF at zero field and its change in the presence of the out-of-plane electric field are shown in Fig. 3. Figures 3(a) and 3(b) show ELF describing the out-of-

plane Ga-N bonds and its change due to the electric field, while Figs. 3(c) and 3(d) provide the same information for the in-plane Ga-N bonds. The Ga-N bonds show a strong ionic characteristic, where very low electron density is found in the middle of the bond, implying very few shared electrons, as shown in Figs. 3(a) and 3(c). The applied external electric field modifies the distribution of electrons and results in an increase in ELF in the middle of the out-of-plane Ga-N bond and a decrease near the nuclei, as shown in Fig. 3(b), implying that the charge density in the bonding region increases, and thus, the ionicity of this out-of-plane Ga-N bond is decreased. In contrast, for the in-plane Ga-N bonds, the ionicity increases with the electric field, which is reflected in the increased charge density near the N atom. It is understood that more ionic bonds usually possess lower bond stiffness and, thus, lead to a lower lattice thermal conductivity,³¹ and thus, the impact of the applied electric field on the bond ionicity in GaN also contributes to the change in the thermal conductivity.

So far, we have analyzed the change in the phonon scattering rates, bond stiffness, and ionicity in the presence of the out-of-plane

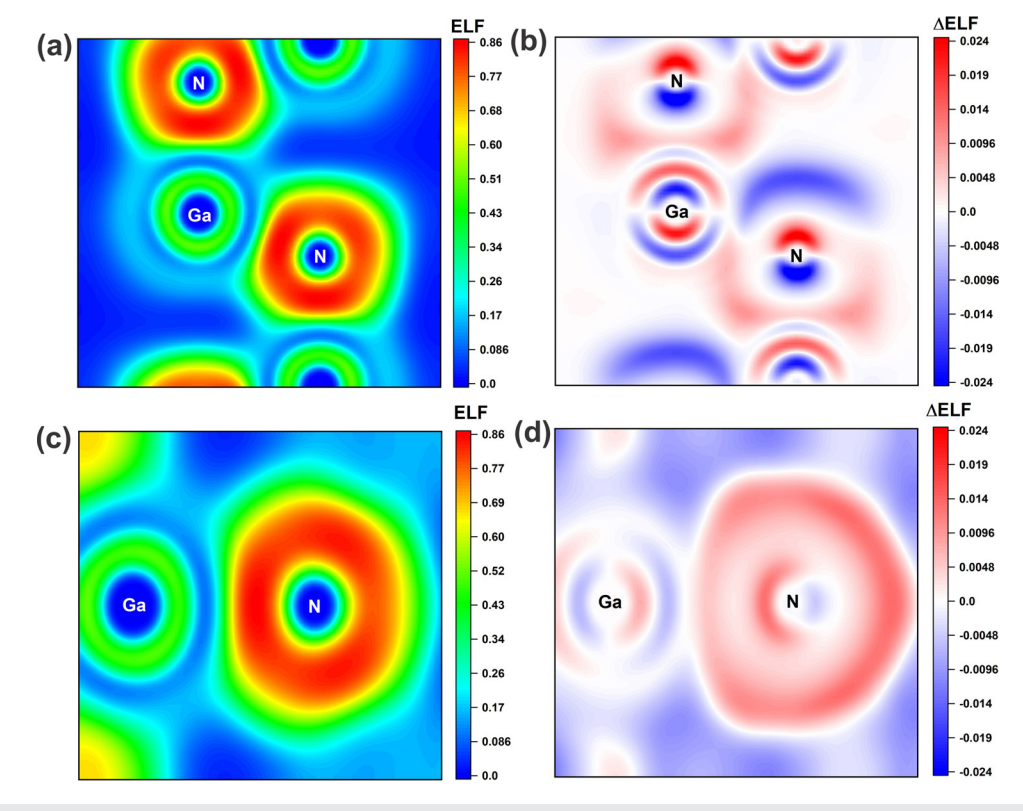


FIG. 3. The electron localization function (ELF) at zero field and its change in the presence of the out-of-plane electric field. [(a) and (b)] A cross section along the (110) surface showing the ELF around out-of-plane Ga–N bonds. [(c) and (d)] A cross section determined by the in-plane Ga–N bond direction and the [110] crystallographic direction, showing the ELF around an in-plane Ga–N bond. The ELF values are coded in the color bars.

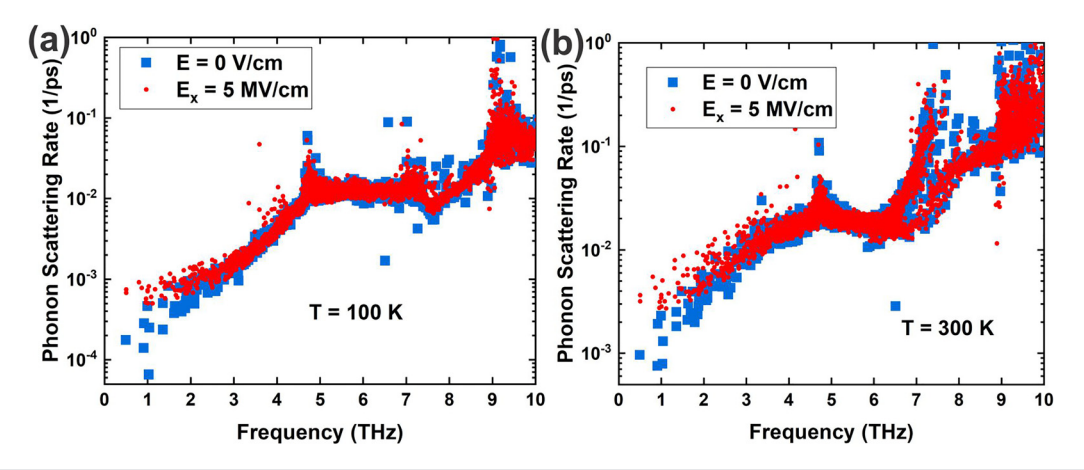


FIG. 4. Calculated phonon—phonon scattering rates at (a) 100 K and (b) 300 K with and without the applied in-plane electric field of 5 MV/cm. The low-frequency acoustic phonons are mostly affected by the symmetry-breaking electric field.

electric field. We conclude that the out-of-plane electric field, under which the crystal symmetry is preserved, increases the thermal conductivity along the out-of-plane direction via reducing the scattering rates of phonons traveling along the out-of-plane direction, enhancing the strength of the Ga–N bonds along the same direction and reducing its ionicity. In the meantime, the out-of-plane electric field decreases the thermal conductivity perpendicular to the electric field through the opposite effects.

When the electric field is applied along the in-plane direction, the thermal conductivities along all directions show a significant reduction. Different from the out-of-plane electric field, under which the crystal symmetry is preserved, the in-plane electric field breaks the crystal symmetry. The space group of the wurtzite GaN crystal structure is P63mc, while after the full lattice relaxation with the in-plane electric field of 5 MV/cm, the space group of the crystal structure becomes P1, indicating the complete absence of any rotation axes, rotary-inversion axes, screw axes, or mirror planes. Due to the symmetry breaking, selection rules for phonon-phonon scatterings imposed by the crystal symmetry are lifted, contributing to more allowed phonon-phonon scattering channels. A recent study found a 20% reduction in the thermal conductivity of GaAs under a small symmetry-breaking strain.³² Since the zone-center phonons possess the same symmetry operations as the full point group of the crystal, low-frequency acoustic phonons near the zone center are expected to be affected more strongly. To verify this effect in GaN with the inplane electric field, we calculate the phonon-phonon scattering rates with or without the field at 100 K and 300 K, which are shown in Fig. 4. The scattering rates of low frequency acoustic phonons in the presence of the in-plane electric field are enhanced compared to the zero-field scattering rates, which contributes to the reduction in the thermal conductivities along all three directions. This effect is more prominent at lower temperatures (we are not reporting the thermal conductivity at 100 K due to the computational cost to obtain a converged thermal conductivity at lower temperatures).

In summary, we demonstrated the impact of a near-breakdown electric field on phonon transport properties of wurtzite GaN through first-principles calculations. We find that the electric field changes the thermal conductivity considerably by affecting the scattering rates of

phonons traveling along different directions, the bond stiffness and ionicity, and the crystal symmetry, depending on the directions of the applied electric field and the thermal conductivity. Our study points out the importance of the field effect on the thermal conductivity of wide-gap semiconductors and contributes to the future development of electrical and thermal co-design strategies of next-generation power electronic devices.³³

See the supplementary material for additional data and figures, as referred to in the main text.

This work is based on research supported by the National Science Foundation under Award No. CBET-1846927. Y.Q. acknowledges the support from the Graduate Traineeship Program of the UCSB NSF Quantum Foundry via the Q-AMASE-i program under Award No. DMR-1906325. This work used the Extreme Science and Engineering Discovery Environment (XSEDE),³⁴ which was supported by National Science Foundation Grant No. ACI-1548562.

DATA AVAILABILITY

The data that support the findings of this study are available from the corresponding author upon reasonable request.

REFERENCES

¹S. Chowdhury and U. K. Mishra, "Lateral and vertical transistors using the AlGaN/GaN heterostructure," IEEE Trans. Electron Devices **60**, 3060–3066 (2013).

²H. Amano, Y. Baines, E. Beam, M. Borga, T. Bouchet, P. R. Chalker, M. Charles, K. J. Chen, N. Chowdhury, R. Chu *et al.*, "The 2018 GaN power electronics roadmap," J. Phys. D: Appl. Phys. 51, 163001 (2018).

³P. Fay, D. Jena, and P. Maki, *High-Frequency GaN Electronic Devices* (Springer, 2020).

⁴Y. Zhang, M. Sun, Z. Liu, D. Piedra, H.-S. Lee, F. Gao, T. Fujishima, and T. Palacios, "Electrothermal simulation and thermal performance study of GaN vertical and lateral power transistors," IEEE Trans. Electron Devices 60, 2224–2230 (2013).

⁵L. Lindsay, D. A. Broido, and T. L. Reinecke, "Thermal conductivity and large isotope effect in GaN from first principles," Phys. Rev. Lett. 109, 095901 (2012).

- ⁶J. Garg, T. Luo, and G. Chen, "Spectral concentration of thermal conductivity in GaN-A first-principles study," Appl. Phys. Lett. 112, 252101 (2018).
- ⁷J.-Y. Yang, G. Qin, and M. Hu, "Nontrivial contribution of Fröhlich electronphonon interaction to lattice thermal conductivity of wurtzite GaN," Appl. hys. Lett. 109, 242103 (2016).
- ⁸G. A. Slack, L. J. Schowalter, D. Morelli, and J. A. Freitas, Jr., "Some effects of oxygen impurities on AlN and GaN," J. Cryst. Growth 246, 287-298 (2002).
- ⁹H. Shibata, Y. Waseda, H. Ohta, K. Kiyomi, K. Shimoyama, K. Fujito, H. Nagaoka, Y. Kagamitani, R. Simura, and T. Fukuda, "High thermal conductivity of gallium nitride (GaN) crystals grown by HVPE process," Mater. Trans. 48, 2782-2786 (2007).
- ¹⁰P. Paskov, M. Slomski, J. Leach, J. Muth, and T. Paskova, "Effect of Si doping on the thermal conductivity of bulk GaN at elevated temperatures-theory and experiment," AIP Adv. 7, 095302 (2017).
- ¹¹Z. Cheng, F. Mu, L. Yates, T. Suga, and S. Graham, "Interfacial thermal conductance across room-temperature-bonded GaN/diamond interfaces for GaN-ondiamond devices," ACS Appl. Mater. Interfaces 12, 8376-8384 (2020).
- ¹²K. R. Bagnall, C. E. Dreyer, D. Vanderbilt, and E. N. Wang, "Electric field dependence of optical phonon frequencies in wurtzite GaN observed in GaN high electron mobility transistors," J. Appl. Phys. 120, 155104 (2016).
- ¹³S. Baroni, S. De Gironcoli, A. Dal Corso, and P. Giannozzi, "Phonons and related crystal properties from density-functional perturbation theory," Rev. Mod. Phys. 73, 515 (2001).
- 14D. A. Broido, M. Malorny, G. Birner, N. Mingo, and D. Stewart, "Intrinsic lattice thermal conductivity of semiconductors from first principles," Appl. Phys. Lett. 91, 231922 (2007).
- ¹⁵L. Lindsay, "First principles Peierls-Boltzmann phonon thermal transport: A topical review," Nanoscale Microscale Thermophys. Eng. 20, 67-84 (2016).
- 16 K. Kunc and R. Resta, "External fields in the self-consistent theory of electronic states: A new method for direct evaluation of macroscopic and microscopic dielectric response," Phys. Rev. Lett. 51, 686 (1983).
- ¹⁷G. Qin, Z. Qin, S.-Y. Yue, Q.-B. Yan, and M. Hu, "External electric field driving the ultra-low thermal conductivity of silicene," Nanoscale 9, 7227-7234 (2017).
- ¹⁸Z. Yang, K. Yuan, J. Meng, and M. Hu, "Electric field tuned anisotropic to isotropic thermal transport transition in monolayer borophene without altering its atomic structure," Nanoscale 12, 19178-19190 (2020).
- ¹⁹J. F. Ihlefeld, B. M. Foley, D. A. Scrymgeour, J. R. Michael, B. B. McKenzie, D. L. Medlin, M. Wallace, S. Trolier-McKinstry, and P. E. Hopkins, "Room-temperature voltage tunable phonon thermal conductivity via reconfigurable interfaces in ferroelectric thin films," Nano Lett. 15, 1791-1795 (2015).

- ²⁰B. M. Foley, M. Wallace, J. T. Gaskins, E. A. Paisley, R. L. Johnson-Wilke, J.-W. Kim, P. J. Ryan, S. Trolier-McKinstry, P. E. Hopkins, and J. F. Ihlefeld, "Voltage-controlled bistable thermal conductivity in suspended ferroelectric thin-film membranes," ACS Appl. Mater. Interfaces 10, 25493-25501 (2018).
- ²¹P. Umari and A. Pasquarello, "Ab initio molecular dynamics in a finite homo-
- geneous electric field, Phys. Rev. Lett. 89, 157602 (2002).

 ²²I. Souza, J. Íñiguez, and D. Vanderbilt, "First-principles approach to insulators in finite electric fields," Phys. Rev. Lett. 89, 117602 (2002).
- ²³X. Wang and D. Vanderbilt, "First-principles perturbative computation of phonon properties of insulators in finite electric fields," Phys. Rev. B 74, 054304 (2006).
- ²⁴P. Giannozzi, S. Baroni, N. Bonini, M. Calandra, R. Car, C. Cavazzoni, D. Ceresoli, G. L. Chiarotti, M. Cococcioni, I. Dabo et al., "QUANTUM ESPRESSO: A modular and open-source software project for quantum simulations of materials," J. Phys.: Condens. Matter 21, 395502 (2009).
- ²⁵D. R. Hamann, "Optimized norm-conserving Vanderbilt pseudopotentials," Phys. Rev. B 88, 085117 (2013).
- 26H. Schulz and K. Thiemann, "Crystal structure refinement of AlN and GaN," Solid State Commun. 23, 815-819 (1977).
- ²⁷K. Esfarjani, G. Chen, and H. T. Stokes, "Heat transport in silicon from firstprinciples calculations," Phys. Rev. B 84, 085204 (2011).
- ²⁸A. Togo, F. Oba, and I. Tanaka, "First-principles calculations of the ferroelastic transition between rutile-type and CaCl2-type SiO2 at high pressures," Phys. Rev. B 78, 134106 (2008).
- 29W. Li, J. Carrete, N. A. Katcho, and N. Mingo, "ShengBTE: A solver of the Boltzmann transport equation for phonons," Comput. Phys. Commun. 185, 1747-1758 (2014).
- ³⁰A. Savin, R. Nesper, S. Wengert, and T. F. Fässler, "ELF: The electron localization function," Angew. Chem., Int. Ed. Engl. 36, 1808-1832 (1997).
- ³¹A. Joffe, "Heat transfer in semiconductors," Can. J. Phys. **34**, 1342–1355 (1956).
- 32A. Vega-Flick, D. Jung, S. Yue, J. E. Bowers, and B. Liao, "Reduced thermal conductivity of epitaxial gaas on si due to symmetry-breaking biaxial strain," Phys. Rev. Mater. 3, 034603 (2019).
- 33J. Tsao, S. Chowdhury, M. Hollis, D. Jena, N. Johnson, K. Jones, R. Kaplar, S. Rajan, C. Van de Walle, E. Bellotti et al., "Ultrawide-bandgap semiconductors: Research opportunities and challenges," Adv. Electron. Mater. 4, 1600501
- 34J. Towns, T. Cockerill, M. Dahan, I. Foster, K. Gaither, A. Grimshaw, V. Hazlewood, S. Lathrop, D. Lifka, G. D. Peterson et al., "XSEDE: Accelerating scientific discovery," Comput. Sci. Eng. 16, 62–74 (2014).